

# Cure Kinetics of Epoxy Resin and Aromatic Diamines

M. Ghaemy, M. Barghamadi, H. Behmadi

Department of Chemistry, Mazandaran University, Babolsar, Iran

Received 30 January 2004; accepted 14 May 2004

DOI 10.1002/app.20960

Published online in Wiley InterScience (www.interscience.wiley.com).

**ABSTRACT:** The kinetics of curing reaction of a diglycidyl ether of a bisphenol-A based epoxy (DGEBA) with 4,4'-diaminostillbene (DAS) and 4,4'-diaminoazobenzene (DAAB) as curing agents are studied by differential scanning calorimetry (DSC) using the isothermal technique. The experimental data show that the cure reaction is autocatalytic in nature, and all kinetic parameters of the curing reaction are determined using a semiempirical equation. The reaction of DGEBA with DAS is faster than that with DAAB under the same conditions

and the activation energies of both systems are higher than those reported for other aromatic diamines. With increasing isothermal temperature and concentration of curing agents the rate constants are increased by the increasing of probability collisions between epoxide and primary amine groups while the activation energies remain constant. © 2004 Wiley Periodicals, Inc. *J Appl Polym Sci* 94: 1049–1056, 2004

**Key words:** curing of polymers; DSC; resins; kinetics

## INTRODUCTION

Linear epoxy resins are converted into three-dimensional crosslinked thermoset networks during cure. The properties of a thermosetting polymer depend on the extent of chemical reactions that take place during cure and the resin morphology. The curing of epoxy resin passes from the liquid state through its gel point, where it is transformed into a rubber, then through the vitrification point, at which it is converted into a glass. Although the chemistry involved in the epoxy curing process is rather complex, understanding the mechanisms and kinetics of the cure reactions is essential for a better knowledge of structure–property relationships. Curing agents such as diamines and anhydrides are useful in most of the important applications of epoxy resins. Aromatic diamines, as curing agents, improve thermal, chemical, and mechanical properties of the cured epoxy resin in comparison with the aliphatic diamines. Various studies, using different experimental techniques, report efforts to evaluate the rate and mechanism of the cure reactions. DSC both in dynamic and isothermal modes has been the most commonly used experimental technique to study kinetics and mechanisms of cure reactions of epoxy resins with different curing agents.<sup>1–11</sup> In these studies, the rate of heat released during cure, measured as a function of time and temperature, was assumed to be directly proportional to the rate of reaction  $d\alpha/dt$ :

$$d\alpha/dt = (1/\Delta H)(dH/dt) \quad (1)$$

The extent of reaction ( $\alpha$ ) was taken to be the heat evolved at a certain time ( $\Delta H_t$ ) divided by the total heat of reaction ( $\Delta H$ ), which is the area under a DSC trace up to time  $t$  divided by the total area of the DSC trace, respectively:

$$\alpha_t = (\Delta H_t)/(\Delta H) \quad (2)$$

In the present study, we have used the isothermal DSC technique to study the cure reaction kinetics of DGEBA with two aromatic diamines, DAS and DAAB, which our literature studies showed to not have been used as curing agents for epoxy resins before. To calculate the kinetic parameters, DSC analysis under isothermal conditions was conducted and the data were introduced to the autocatalytic-like kinetic model.

## EXPERIMENTAL

### Apparatus

A Perkin–Elmer differential scanning calorimeter (DSC-4) was used to monitor the exothermic thermograms of the crosslinking reaction. The instrument was first calibrated with pure indium for thermal response with the heat of fusion and the temperature with the melting point. For nonisothermal DSC, a baseline adjustment was obtained first with empty DSC pans. For isothermal DSC, the sample was loaded into the DSC cell at room temperature and then it was raised quickly to the isothermal temperature. DSC experiments were carried out under atmospheric pressure and an identical empty cell was taken as reference. The infrared spectrometer used was Unicam SP

Correspondence to: M. Ghaemy (ghaemy@umz.ac.ir).

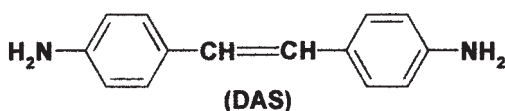
1100. The IR spectra of the synthesized curing agents were taken using KBr pellets. The H-NMR spectra were recorded with a Varian EM 360 at 60 MHz.

## Materials

The epoxy compound used in the study was a diglycidyl ether of a bisphenol A-based epoxy (DGEBA) provided from Shell Chemical Co., Epon 828, with an epoxy equivalent weight (eew) of 185. Other compounds such as *p*-nitrotoluene, hydrazinehydrate 85%, diethylene glycol, *p*-aminoacetanilide, sodium perborate tetrahydrate, boric acid, and methanol were obtained from Fluka and used without further purification.

## Synthesis

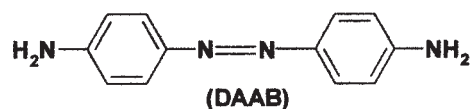
Compound 4,4'-diaminostilben (DAS) was synthesized according to the procedure given in the literature.<sup>12</sup> To a solution of 10.96 g (0.08 mol) *p*-nitrotoluene in 160 mL diethyleneglycol, 21.5 mL hydrazinehydrate 85% and 24 g KOH were added and the mixture was heated under reflux. After 30 min the condenser was removed and the reaction temperature increased to 200°C to distill out the water produced during the reaction, then the mixture was refluxed for another 3 h. The reaction mixture was cooled and the brown solid was collected on a filter paper, washed with distilled water, and recrystallized in ethanol. The brown solid dried under reduced pressure; the yield was 30% and the product had a melting range of 225–228°C. The results of H-NMR and IR spectroscopy of the product are the same as given in the literature.



Compound 4,4'-diaminoazobenzene (DAAB) was synthesized in two stages according to the procedure given in the literature.<sup>13</sup> In the first stage, compound 4,4'-bis(acetamido)azobenzene (**I**) was prepared in a 1-L three-necked round-bottomed flask equipped with a thermometer, mechanical stirrer, and a reflux condenser, where 29 g (0.19 mol) of *p*-aminoacetanilide, 40 g (0.26 mol) of sodium perborate tetrahydrate, 500 mL of glacial acetic acid, and 10 g (0.16 mol) of boric acid were placed. The mixture was heated to 60°C and was held at this temperature with stirring for 6 h during which the solids dissolved first but began to separate later. The mixture was cooled to room temperature and the yellow product was collected on a filter paper and washed several times with distilled water until the washing was neutral to pH paper and then dried in an oven at 110°C. The yield of (**I**), m.p.

285–295°C, was 14.8 g (51%) and it was used directly for the second step.

DAAB was prepared in a 500-mL round-bottomed flask equipped with a reflux condenser and a magnetic stirrer, where the total yield of the first step product (**I**), 150 mL of methanol, and 150 mL of 6*N* hydrochloric acid were placed. The reaction mixture was heated under reflux for 90 min. After cooling the reaction mixture, the violet solid was suspended in 500 mL of distilled water with stirring and was slowly neutralized by the addition of 2.5*N* sodium hydroxide. The product was collected on a filter paper, washed with distilled water, and dried under reduced pressure. The yield of the product, m.p. 236–239°C, was 12 g (about 56%). The H-NMR and FTIR spectra provided enough evidence for the structures of the DAAB compound.



## Sample preparation

The stoichiometric amounts of the curing agents were calculated through the number of active amino hydrogens in DAS and DAAB. For instance, DAS with a molar mass of 210 g/mol (212 g/mol for DAAB), contains 4 active hydrogen atoms. Therefore, 1 mole of active hydrogen atoms represents 52.5 g of DAS. This figure is in the stoichiometric equivalent of the eew and, hence, for 185 g of DGEBA, 52.5 g DAS (or 53 g DAAB) as curing agent is required. Samples of DGEBA, containing the required amounts of curing agents, were completely mixed by stirring at room temperature. A certain amount of the uniform viscous liquid was put into a DSC sample pan and covered with an aluminum lid and closed tightly under pressure. The sample pan was placed in the DSC sample cell at ambient temperature and an empty pan was also placed in the DSC reference cell. The temperature was then increased at a controlled rapid rate (323 K/min) to the required temperature and the isothermal tests were carried out under atmospheric pressure. The isothermal temperatures for each curing agent at a particular concentration were determined from the corresponding dynamic thermograms. The temperatures were selected from an interval defined between 283 K below the onset of cure and a point midway to the peak maximum. The selected temperatures in each interval were 283 K apart. The reaction was considered complete when the rate curve leveled off to the baseline. The complete heat of cure was estimated as the area under the cure exotherm, measured with a planimeter.

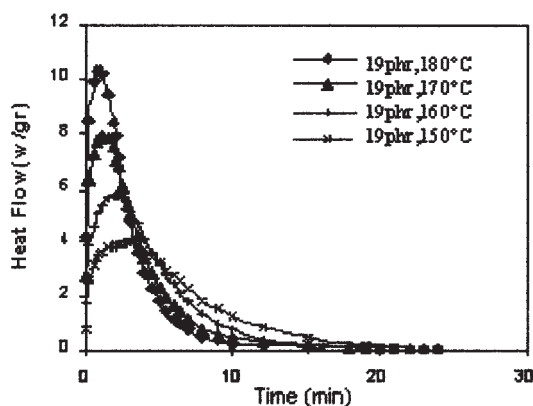


Figure 1 Isothermal DSC thermograms for DGEBA + DAS.

## RESULTS AND DISCUSSION

The isothermal DSC experiments were performed in the temperature ranges of 150–180 and 175–205°C for DGEBA/DAS and DGEBA/DAAB systems, respectively. Figure 1 shows some typical isothermal DSC curves for the studied systems at a specific concentration. Table I presents some of the data extracted from isothermal DSC thermograms. In all DSC thermograms, the rate of heat generation ( $dH/dt$ ) was found to exhibit a maximum when plotted as a function of time. If the cure reaction is the only thermal event, then according to eq. (1) the heat released during the cure reaction ( $dH/dt$ ) is directly proportional to the rate of reaction ( $d\alpha/dt$ ). Consequently, the reaction rate also passes through a maximum and then decreases with time. The maximum heat generation is reached in a shorter time at a definite concentration with increasing isothermal temperature. The maximum heat flow increases with increasing isothermal

temperature and concentration of curing agent, as can be seen in Table I. Total enthalpies were 179.4 and 135.7 kJ for each mole of DAAB and DAS, respectively, in the mixture with the resin. Other researchers<sup>5</sup> have also reported a higher heat of reaction for DGEBA cured with diamino diphenyl sulfone (DDS). The higher enthalpy of the DGEBA/DAAB system in comparison with the DGEBA/DAS system can probably be attributed to two reasons: (1) the catalyzing effect of the azo group, which causes other reactions such as etherification to occur and (2) the decomposition of DAAB, which can slightly start at the isothermal temperatures.

It is necessary to use an equation expressing the rate of conversion ( $d\alpha/dt$ ) as a function of  $\alpha$  and temperature. The cure kinetics has been described by both  $n$ th order<sup>14–18</sup> and autocatalytic mechanisms.<sup>4–11</sup> For thermosets that follow  $n$ th order kinetics,  $d\alpha/dt$  is proportional to the fraction of material unreacted ( $1 - \alpha$ ) and expressed<sup>4</sup> as follows:

$$d\alpha/dt = K(1 - \alpha)^n \quad (3)$$

where  $n$  is the reaction order and  $K$  is the specific rate constant. Systems obeying  $n$ th order kinetics will obviously have the maximum reaction rate at  $t = 0$ .

The behavior of the reaction rate as a function of time, which shown in Figure 1 is characteristic of chemical reactions in which products act as catalysts for the continuing reaction and which are referred to as the autocatalytic reactions. An autocatalyzed thermoset usually has its maximum heat evolution at 30–40% conversion. Authors<sup>5–9</sup> who have studied the autocatalytic isothermal curing reaction of epoxy resin all used the following equation:

$$d\alpha/dt = k' \alpha^m (1 - \alpha)^n \quad (4)$$

TABLE I  
Representation of Some of the Data Extracted from Isothermal DSC Curves

| Amine | Concentration (phr) | Temperature (°C) | Maximum heat flow (J g <sup>-1</sup> s <sup>-1</sup> ) | Time of maximum heat flow (s) | Enthalpy (Jg <sup>-1</sup> ) |
|-------|---------------------|------------------|--|-------------------------------|------------------------------|
| DAS   | 19                  | 150              | 3.99   | 180                           | -473.9                       |
| DAS   | 19                  | 160              | 5.76   | 120                           | -479.9                       |
| DAS   | 19                  | 170              | 7.84   | 72                            | -481.8                       |
| DAS   | 19                  | 180              | 10.25  | 60                            | -482.1                       |
| DAS   | 29                  | 150              | 6.54   | 168                           | -646.3                       |
| DAS   | 29                  | 160              | 9.63   | 108                           | -647.8                       |
| DAS   | 29                  | 170              | 13.61  | 60                            | -646.8                       |
| DAS   | 29                  | 180              | 16.97  | 48                            | -645.2                       |
| DAAB  | 19                  | 175              | 5.47   | 210                           | -632.1                       |
| DAAB  | 19                  | 185              | 6.38   | 168                           | -635.8                       |
| DAAB  | 19                  | 195              | 8.24   | 72                            | -636.8                       |
| DAAB  | 19                  | 205              | 12.57  | 60                            | -638.1                       |
| DAAB  | 29                  | 175              | 9.74   | 150                           | -843.6                       |
| DAAB  | 29                  | 185              | 14.29  | 90                            | -845.0                       |
| DAAB  | 29                  | 195              | 20.17  | 60                            | -847.9                       |
| DAAB  | 29                  | 205              | 31.24  | 30                            | -849.7                       |

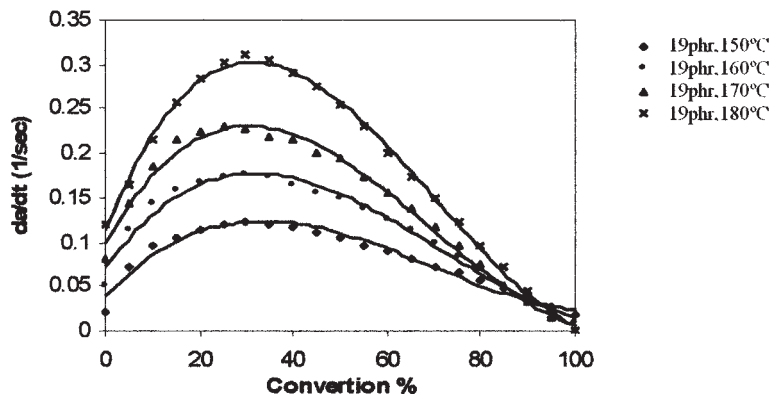


Figure 2 Reaction rate versus conversion (%) for DGEBA + DAS.

where  $m$  and  $n$  are the reaction orders and  $k'$  is the specific reaction rate constant. According to this model, the rate is zero initially and attains a maximum value at some intermediate conversion. The initial rate of an autocatalytic reaction is not necessarily zero, since there is a possibility that reactants can be converted into products via alternative paths, only one of which is autocatalytic. During the isothermal studies, the curing reaction shows a marked autocatalytic behavior and that may be successfully described by the following equation:<sup>19</sup>

$$d\alpha/dt = (k_1 + k_2\alpha^m)(1 - \alpha)^n \quad (5)$$

A good fit to experimental data of the studied reaction systems was obtained by using this model with four kinetic parameters ( $k_1$ ,  $k_2$ ,  $m$ , and  $n$ ). Figure 2 shows plots of reaction rate,  $d\alpha/dt$ , versus conversion,  $\alpha$ , for the isothermal DSC thermograms presented in Figure

1. At any given time, the extent of reaction was seen to increase as both temperature and concentration of curing agents were increased. The plots of  $d\alpha/dt$  against time, which are similar to the plots given in Figure 1, show a maximum reaction rate at time greater than zero, thereby negating simple  $n$ th order kinetics. The maximum rate for the present systems is observed at conversions around  $\sim 40\%$ , as expected for an autocatalytic reaction. The isothermal curves obtained in the present study always gave a nonzero initial reaction rate, which has been attributed to certain reactions that are dominant only in the early stages of cure. Taking into account the above observations, eq. (5), representing autocatalytic systems, was chosen to test the rate data of the present systems. At the start of the cure reaction ( $t = 0$ ,  $\alpha = 0$ ), eq. (5) simplifies to:

$$[d\alpha/dt]_{t=0} = k_1. \quad (6)$$

TABLE II  
Initial and Final Values of Four Kinetic Parameters

| Amine | Concentration (phr) | Temperature (°C) | $K_1$ ( $s^{-1}$ ) | Initial $n$ | Final $n$ | Initial $m$ | Final $m$ | Initial $Lnk_2$ ( $s^{-1}$ ) | Final $Lnk_2$ ( $s^{-1}$ ) |
|-------|---------------------|------------------|--------------------|-------------|-----------|-------------|-----------|------------------------------|----------------------------|
| DAS   | 19                  | 150              | 0.021              | 0.623       | 0.862     | 0.469       | 0.515     | -1.452                       | -1.33                      |
| DAS   | 19                  | 160              | 0.051              | 0.839       | 1.052     | 0.536       | 0.583     | -1.023                       | -0.875                     |
| DAS   | 19                  | 170              | 0.082              | 1.097       | 1.298     | 0.634       | 0.673     | -0.561                       | -0.431                     |
| DAS   | 19                  | 180              | 0.131              | 1.114       | 1.352     | 0.711       | 0.830     | -0.324                       | 0.040                      |
| DAS   | 29                  | 150              | 0.040              | 0.843       | 1.113     | 0.554       | 0.657     | -1.268                       | -0.990                     |
| DAS   | 29                  | 160              | 0.085              | 0.928       | 1.166     | 0.686       | 0.806     | -0.642                       | -0.500                     |
| DAS   | 29                  | 170              | 0.120              | 1.194       | 1.470     | 0.717       | 0.793     | -0.686                       | 0.06                       |
| DAS   | 29                  | 180              | 0.171              | 1.262       | 1.702     | 0.877       | 0.981     | 0.225                        | 0.3653                     |
| DAAB  | 19                  | 175              | 0.001              | 0.908       | 1.242     | 0.413       | 0.412     | -1.443                       | -1.30                      |
| DAAB  | 19                  | 185              | 0.008              | 0.953       | 1.262     | 0.457       | 0.567     | -1.221                       | -0.874                     |
| DAAB  | 19                  | 195              | 0.018              | 1.111       | 1.345     | 0.456       | 0.455     | -0.534                       | -0.48                      |
| DAAB  | 19                  | 205              | 0.022              | 0.905       | 1.355     | 0.477       | 0.460     | -0.453                       | -0.11                      |
| DAAB  | 29                  | 175              | 0.007              | 0.920       | 1.218     | 0.497       | 0.493     | -1.012                       | -0.77                      |
| DAAB  | 29                  | 185              | 0.013              | 1.047       | 1.193     | 0.497       | 0.494     | -0.525                       | -0.35                      |
| DAAB  | 29                  | 195              | 0.020              | 1.085       | 1.237     | 0.507       | 0.503     | -0.136                       | 0.05                       |
| DAAB  | 29                  | 205              | 0.027              | 1.218       | 1.411     | 0.643       | 0.639     | 0.390                        | 0.437                      |



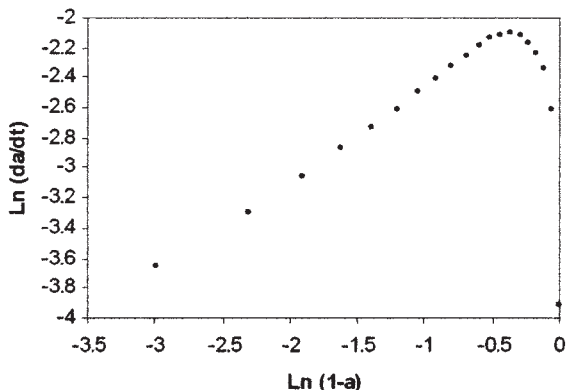


Figure 3 Graphic representation of eq. (6) for DGEBA + DAS (19 phr, 150°C).

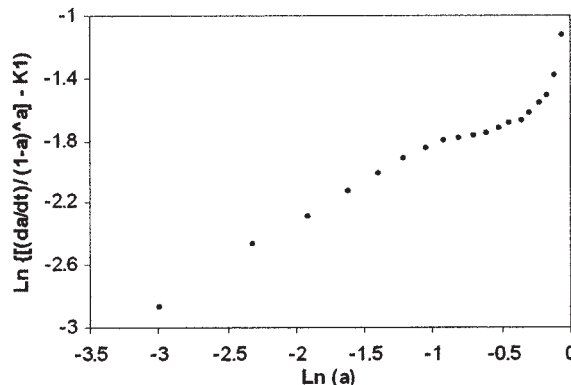


Figure 4 Graphic representation of eq. (7) for DGEBA + DAS (19 phr, 150°C).

The kinetic rate constant  $k_1$  was determined directly from isothermal reaction rate curves by extrapolating to zero time and is given in Table II.

There are different calculative approaches, which have been applied by other researchers<sup>8,9</sup> for determination of the kinetic parameters in eq. (5). Those methods were based on assumptions, which are limited to reactions where the total reaction rate order is known. The best calculative approach is the graphic-analytical method applied by Kenny.<sup>20</sup> In the present study, we have also used this approach for calculating parameters  $m$ ,  $n$ , and  $k_2$ .

By taking the logarithm of eq. (5) it yields

$$\ln(d\alpha/dt) = \ln(k_1 + k_2\alpha^m) + n \ln(1 - \alpha). \quad (7)$$

Figure 3 represents a typical plot of  $\ln(d\alpha/dt)$  as a function of  $\ln(1 - \alpha)$  for the DGEBA/DAS system at a specific concentration and temperature. It can be concluded from eq. (7) that the slope of the linear behavior observed when  $\alpha \rightarrow 1$  is the reaction order  $n$ . Equation (7) can also be rearranged in the following form:

$$\ln\{[(d\alpha/dt)/(1 - \alpha)^n] - k_1\} = \ln k_2 + m \ln \alpha \quad (8)$$

Figure 4 represents a typical plot of the first term of eq. (8) as a function of  $\ln \alpha$  for the same experimental results shown in Figure 3. The first term of eq. (8) has been calculated using previously computed  $k_1$  and  $n$  values. The reaction order,  $m$ , and the kinetic constant,  $k_2$ , were calculated, respectively, from the slope and intercept of the linear portion of the graphic representation of Figure 6. A first set of parameter values was obtained using the procedure described above. However, to obtain more values, an interactive procedure can be applied. Equation (8) can be rearranged again to give

$$\ln[(d\alpha/dt)/(k_1 + k_2\alpha^m)] = n \ln(1 - \alpha). \quad (9)$$

After  $k_2$  and  $m$  have been evaluated using eq. (8), the left part of eq. (9) can be calculated and plotted as a function of  $\ln(1 - \alpha)$ . Figure 5 represents a typical plot of the first term of eq. (9) as a function of  $\ln(1 - \alpha)$ . The new value of the reaction order  $n$  obtained from the slope of the linear portion of this plot is close to the one obtained previously. Equation (8) can be used again to obtain neat values of  $m$  and  $k_2$  that are close to the previous ones. These new values are applied again in eq. (9). This interactive procedure was repeated until the obtained values for  $n$ ,  $m$ , and  $k_2$  showed less than 1% difference between subsequent calculations. Therefore, the final values of  $n$ ,  $m$ , and  $k_2$  of eq. (5) obtained by this procedure are reported in Table II. For all formulations of the present systems, the values of  $m$  and  $n$  appear to increase somewhat with increasing isothermal temperatures. There are some contradictions in the value of  $m$  in relation with the temperature. Other researchers have also reported that the value of  $m$  for all the studied formulations increased with increasing temperature,<sup>5,8</sup> while others reported a decrease in  $m$  with increasing temperature.<sup>9</sup> We have also reported an increase in  $m$  with increasing temper-

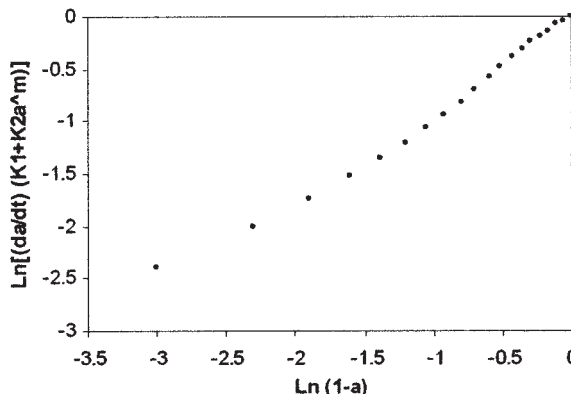


Figure 5 Graphic representation of eq. (8) for DGEBA+DAS (19 phr, 150°C).

TABLE III  
Average Values of  $m$  and  $n$  for the DGEBA/Amines System Studied

| Amine | Concentration (phr) | Average $n$ | Average $m$ | $m + n$ |
|-------|---------------------|-------------|-------------|---------|
| DAS   | 19                  | 1.1408      | 0.6503      | 1.7911  |
| DAS   | 29                  | 1.3629      | 0.8092      | 2.1721  |
| DAAB  | 19                  | 1.3011      | 0.4725      | 1.7736  |
| DAAB  | 29                  | 1.2682      | 0.5323      | 1.8005  |

ature for the same resin cured with  $\text{BF}_3$ -diamine complexes.<sup>21</sup> The value of  $m$  was also reported<sup>22,23</sup> to be independent of temperature, but changed as a function of type (chemistry) of the formulations. The values of  $m$  and  $n$  of the present systems also changed as a function of the type of curing agent, as can be seen in Table II. The average values of  $m$  and  $n$  for the present systems are given in Table III. The overall reaction order for both systems approximates to 2. This is in agreement with the previous results reported for DGEBA cured with aromatic diamine<sup>5</sup> and also for TGDDM/DDS formulations.<sup>8</sup> These latter authors found that the error between the predicted values of the rate and those obtained from the data was minimized when the value of  $(m + n)$  was about 2. As reported in the literature,<sup>24</sup> the epoxide ring opening follows a second order mechanism with aliphatic amines. A reaction order between 1 and 2 is observed in the ring opening by acidic media, where the attachment of the weaker nucleophile is assisted by protonation of the oxirane.<sup>25</sup> In the case of aromatic amines, usually weaker than aliphatic, the ring opening reaction appears to be catalyzed by hydrogen donor groups present in the system and explains the value obtained for the kinetic exponent ( $n = 1.1$ – $1.3$ ). This reaction may be described as a catalytic ring opening by the primary amino groups, involving a ternary transition state amino–epoxide–hydrogen donor present in the reaction medium. A true autocatalytic ring opening reaction involves a primary or secondary amine, an epoxide, and a hydroxyl group formed *in situ* by the opening of the first epoxy ring. The kinetic exponent ( $m$ ) represents the quantitative measure of how much of the subsequent curing reactions follow the autocatalytic path. The observed dependence of  $m$  on the curing temperature points out formation of low energy cyclic transition state between amine–epoxide–hydrogen donor groups. A departure from the stoichiometric ratio (formulation containing 19 phr curing agents) decreases the rate of the curing reaction; the difference in the values of  $k_1$  and  $k_2$  was quite noticeable.

Activation energies,  $E_a$ , can be calculated using Arrhenius-type behavior:

$$K = A \exp(-E_a/RT). \quad (10)$$

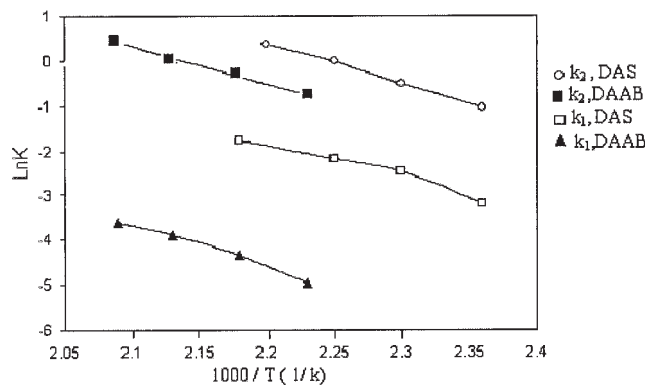


Figure 6 Arrhenius plots for DGEBA/hardeners systems.

By taking the logarithm of eq. (10) it yields

$$\ln k = \ln A - E_a/RT. \quad (11)$$

The temperature dependence of  $k_1$  and  $k_2$  are shown in Figure 6, which represent linear plots of  $\ln k$  versus  $1/T$  for both systems at the stoichiometric ratios. There were fluctuations in the values of the point of initiation of reaction, and such fluctuations are believed to be responsible for the observed deviations of  $k_1$  from the Arrhenius relation. On the other hand, the temperature dependence of the reaction rate constant  $k_2$  fits better the classical Arrhenius form. The average energies of activation based on the rate constant  $k_2$  for both systems are given in Table IV. The activation energies remained constant with a decrease in concentration of curing agents while the frequency factor decreased. As was seen before, the rate of polymerization increases with increasing concentration of the curing agent. This is accomplished through the effect of concentration on rate constant  $k_2$  and, according to the Arrhenius equation, an increase in rate constant must be accompanied by a decrease in activation energy or an increase in frequency factor. Since any change in activation energy is negligible, increase in frequency factor with increase in concentration of curing agent is the main effective factor on the rate of the reaction. The average activation energies based on the rate constant  $k_1$  are 17.5 and 18.8 kcal/mol and based on the rate constant  $k_2$  are 16.8 and 17.1 kcal/mol for

TABLE IV  
Values of Activation Energy and Frequency Factor of DGEBA/Amines System Based on Rate Constants  $k_2$

| Curing agent | Concentration (phr) | $A \times 10^6$ ( $\text{s}^{-1}$ ) | $E_a$ (kcal mol <sup>-1</sup> ) |
|--------------|---------------------|-------------------------------------|---------------------------------|
| DAS          | 19                  | 224                                 | 17.3                            |
| DAS          | 29                  | 263                                 | 16.8                            |
| DAAB         | 19                  | 48                                  | 16.9                            |
| DAAB         | 29                  | 107                                 | 17.1                            |

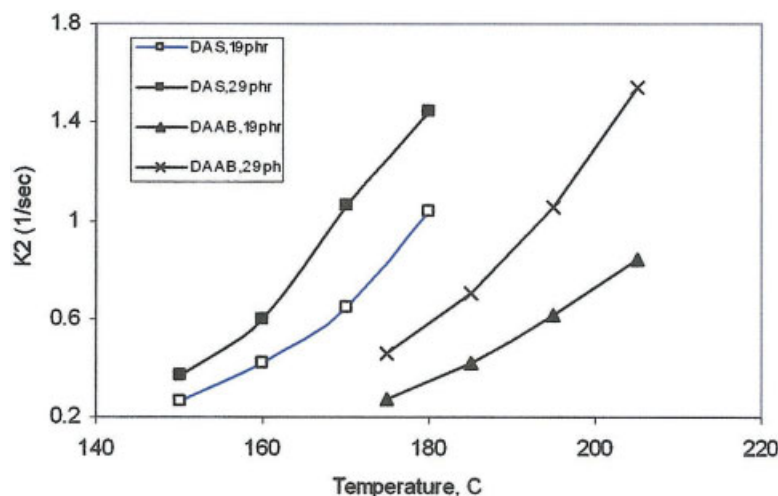


Figure 7 Plots of temperature dependence of reaction rate constant.

DGEBA/DAS and DGEBA/DAAB systems, respectively, at the stoichiometric ratio. The activation energies of the present systems are higher than those reported in the literature for the same resin but with other aromatic diamines, such as 14 kcal/mol,<sup>4</sup> 13.5 kcal/mol,<sup>5</sup> and 12 kcal/mol<sup>26</sup> with ethylene diamine, *m*-phenylene diamine, and diamino cyclohexane, respectively. It is worth mentioning here that our higher activation energy can be due to the fact that the nucleophilic activity of the amino groups in DAS and DAAB molecules is reduced because of the presence of electron withdrawing groups, such as  $-N=N-$  and  $-CH=CH-$ . According to the suggested mechanism for autocatalytic reaction,<sup>2</sup> formation of the ternary complex of amine-epoxide-hydrogen donor will probably have higher activation energy because of the rigid rod-like molecules of DAS and DAAB and the weaker nucleophilic activity of the amino groups in these molecules. The reaction rate constants  $k_2$  and  $k_1$  of the DGEBA/DAS system at any specific concentration and isothermal temperature are also higher than those of the DGEBA/DAAB system, as can be seen in Table II and Figure 7. This also indicates that the reactivity of DAAB molecules as curing agents is lower than DAS molecules. The lower nucleophilic activity of the amino groups in DAAB is due to the fact that the azo group ( $-N=N-$ ) is a stronger electron withdrawing group and thus reduces the rate of nucleophilic attack of the amino group on the oxirane. The lower reactivity of DAAB in comparison with DAS, for the same stoichiometric ratio and isothermal temperature, can also be observed in Table I, where analogous results for both systems showed that the time of maximum heat flow for the DGEBA/DAS system is shorter than that for the DGEBA/DAAB system.

## CONCLUSION

The results obtained from isothermal DSC experiments showed that the rate of reaction was proportional to the heat flow. At any given time, the extent of reaction was seen to increase as both temperature and concentration of curing agents increased.

A four-parameter semiempirical equation for autocatalytic systems containing two rate constants ( $k_1$  and  $k_2$ ) and two reaction orders ( $m$  and  $n$ ) provided a good fit to the experimental data. The overall reaction order of the curing of DGEBA with DAS and DAAB as curing agents was 2. The average activation energy of these systems based on both rate constants was about  $\sim 17.5$  kcal/mol, which is higher than those reported for the same resin with other aromatic diamines ( $\sim 14$  kcal/mol). This was suggested to be due to the fact that rigid rod-like molecules of the present curing agents and also lower nucleophilic activity of their amino groups are responsible for higher activation energy for the formation of the cyclic transition state. The higher nucleophilic activity of DAS in comparison with DAAB can also be responsible for the higher rate of reaction of this curing agent with epoxy resin.

## References

- Chen, C. S.; Pearce, E. M. *J Appl Polym Sci* 1989, 37, 1105.
- Wasserman, S.; Joharei, G. *J Appl Polym Sci* 1993, 48, 905.
- Hamerton, I.; Hay, J.; Herman, H.; Howlin, B. J.; Jepson, P.; Gillies, D. G. *J Appl Polym Sci* 2002, 84, 2411.
- Riccardi, C. C.; Adabbo, H. E.; Williams, R. J. J. *J Appl Polym Sci* 1984, 29, 2481.
- Moroni, A.; Mijovic, J.; Pearce, E.; Foun, C. C. *J Appl Polym Sci* 1986, 32, 3761.
- Nunez, L.; Fraga, F.; Castro, A.; Nunez, M. R.; Villanueva, M. *J Appl Polym Sci* 2000, 75, 291.
- Khana, U.; Chanada, M. *J Appl Polym Sci* 1993, 49, 319.
- Mijovic, J.; Kim, J.; Slaby, J. *J Appl Polym Sci* 1984, 29, 1449.

9. Boey, F. Y. C.; Qiang, W. *Polymer* 2000, 41, 2081.
10. Kiran, E.; Iyer, R. *J Appl Polym Sci* 1994, 51, 353.
11. Tai-Shung, C. *J Appl Polym Sci* 1974, 14, 23.
12. Huang-Minlon; *J Am Chem Soc* 1984, 70, 2802.
13. Santurri, P.; Robbins, F.; Stubbings, R. *Organic Synthesis*, CV5; Baumgarten, H. E., Ed.; John Wiley and Sons: New York, 1973; p. 341.
14. Acitelli, M. A.; Prime, R. B.; Scatt, E. *Polymer* 1971, 12, 335.
15. Donellan, T.; Roylane, D. *Polym Eng Sci* 1982, 22, 821.
16. Schneider, N. S.; Sprous, J. F.; Hagnauer, G. L.; Gillham, J. K. *Polym Eng Sci* 1979, 19, 304.
17. Prime, R. B. *Anal Calorim* 1970, 2, 201.
18. Prime, R. B. *Polym Eng Sci* 1973, 13, 453.
19. Kamal, M. R. *Polym Eng Sci* 1974, 14, 23.
20. Kenny, J. M. *J Appl Polym Sci* 1994, 51, 761.
21. Ghaemy, M.; Khandani, M. H. *Eur Polym Mater* 1998, 34, 477.
22. Kamal, M. R.; Sourour, S.; Ryan, M. *Soc Plast Eng Tech Paper* 1973, 19, 187.
23. Sourour, S.; Kamal, M. R. *Thermochim Acta* 1976, 14, 41.
24. Smith, I. T. *Polymer* 1961, 2, 95.
25. Gould, E. S. *Mechanisms and Structure in Organic Chemistry*; Holt, Rinehart and Winston: New York, 1959; p. 291.
26. Frago, F.; Burgo, S.; Numez, E. R. *J Appl Polym Sci* 2001, 82, 3366.